Sex-Specific Effects of Microglia-Like Cell Engraftment During Experimental Autoimmune Encephalomyelitis

Jinming Han (✉ jinming.han@ki.se)
Karolinska Institutet
Keying Zhu
Karolinska Institutet
Kai Zhou
Karolinska Institutet
Ramil Hakim
Karolinska Institutet
Sreenivasa Raghavan Sankavaram
Karolinska Institutet
Klas Blomgren
Karolinska Institutet
Harald Lund
Karolinska Institutet
Xing-Mei Zhang
Karolinska Institutet
Robert A. Harris
Karolinska Institutet

Research

Keywords: Microglia depletion, Microglia repopulation, Monocytes, Neuroinflammation, Experimental Autoimmune Encephalomyelitis

Posted Date: May 8th, 2020

DOI: https://doi.org/10.21203/rs.3.rs-26029/v1

Abstract

Background

Multiple Sclerosis (MS) is a chronic neuroinflammatory disorder of the central nervous system (CNS) that usually presents in young adults and predominantly in females. Microglia, a major resident immune cell in the CNS, are critical players in both CNS homeostasis and disease. We have previously demonstrated that microglia can be efficiently depleted by the administration of tamoxifen in *Cx3cr1*$^{CreER/+}$*Rosa26*$^{DTA/+}$ mice, with ensuing repopulation deriving from both the proliferation of residual CNS resident microglia and the engraftment of peripheral monocyte-derived microglia-like cells.

Methods

Tamoxifen was administered to *Cx3cr1*$^{CreER/+}$*Rosa26*$^{DTA/+}$ and *Cx3cr1*$^{CreER/+}$ female and male mice. Experimental autoimmune encephalomyelitis (EAE), a widely used animal model of MS, was induced by active immunization with myelin oligodendrocyte glycoprotein one month after tamoxifen injections in *Cx3cr1*$^{CreER/+}$*Rosa26*$^{DTA/+}$ mice and *Cx3cr1*$^{CreER/+}$ mice, a time point when the CNS niche was colonized by microglia derived from both CNS microglia and peripherally-derived macrophages. CNS myeloid cell compositions during acute and chronic EAE were measured by flow cytometry.

Results

We demonstrate that engraftment of microglia-like cells following microglial depletion exacerbated EAE in *Cx3cr1*$^{CreER/+}$*Rosa26*$^{DTA/+}$ female mice as assessed by clinical symptoms and the expression of CNS inflammatory factors, but these findings were not evident in male mice. Higher major histocompatibility complex class II expression and cytokine production in the female CNS contributed to the sex-dependent EAE severity in mice following engraftment of microglia-like cells.

Conclusion

The engraftment of microglia-like cells following microglial depletion exacerbated EAE in females. An underestimated yet marked sex-dependent microglial activation pattern may exist in the injured CNS during EAE.

Introduction

Multiple Sclerosis (MS) is a complex neuroinflammatory disorder of the central nervous system (CNS) associated with progressive and irreversible neurological dysfunctions [1]. As specialized resident innate immune cells in the CNS, microglia provide neurotrophic support, contribute to normal myelinogenesis, synaptic pruning and refine neural circuits, thereby maintaining CNS homeostasis [2–5]. Microglial activation is widely noted in numerous neurological diseases such as MS [6, 7], and comprehensive MS genomic mapping also highlighted the inferred contribution of brain resident microglia [8]. Microglial-

induced neuroinflammation plays a fundamental role in both the occurrence and progression of MS [8, 9]. It has recently become clear that homeostatic microglia are in fact nearly lost in active and slowly expanding MS lesions, whereas long-lived microglia exhibited an intermediate phenotype between pro-inflammatory and anti-inflammatory states in later stages of MS [10]. The complexity of CNS innate cell populations may be amplified significantly in the context of neuroinflammation, reflecting heterogeneous responses by microglia and subsequent recruitment of diverse circulating immune cells into the injured CNS [11, 12].

How microglia could be precisely targeted for optimal therapeutic efficacy has gained much-deserved attention recently [13–15]. Microglia can be depleted experimentally through genetic targeting, conditional genetic targeting or pharmacological therapies as we previously reviewed [16, 17]. Several investigations have utilized transgenic microglial depletion animal models have been utilized such as tamoxifen-induced *Cx3cr1*$^{\mathrm{CreER}}$ mice in which diphtheria toxin receptor (DTR) is expressed upon Cre-mediated recombination (*Cx3cr1*^{creER}*DTR* mice) [18],and *Cx3xr1*$^{CreER/+}$*Csf1r*$^{Flox/Flox}$ mice that target the CSFR1 receptor, CSFR1 being critical for microglia well-being [19]. Newly repopulated microglia following both genetic and pharmacological depletion exhibit a neuroprotective phenotype and can contribute to recovery after brain injury [20]. More recently, we have demonstrated that microglia can be efficiently depleted by the administration of tamoxifen in *Cx3cr1*$^{CreER/+}$*Rosa26*$^{DTA/+}$ mice, this being followed by simultaneous long-term repopulation of the empty microglial niche from both CNS residual microglia and circulating monocytes [21–23]. We and others have proven that circulating monocytes can engraft the CNS and then give rise to long-lived microglia-like cells [21, 24]. However, the functionality of cellular therapeutic effects of the engraftment of microglia-like cells during MS is poorly understood.

We hypothesized that the engraftment of microglia-like cells following experimental microglia depletion could be beneficial for resolving ongoing neuroinflammation and promoting disease recovery in experimental autoimmune encephalomyelitis (EAE). Immunizing both female and male *Cx3cr1*$^{CreER/+}$*Rosa26*$^{DTA/+}$mice with myelin oligodendrocyte glycoprotein (MOG) to induce EAE, we report that exacerbated EAE in female mice may result from the engraftment of microglia-like cells. This sex-dependent EAE severity following microglia-like cell engraftment may partially be due to higher major histocompatibility complex class II (MHCII) expression and cytokine production in the female CNS.

Methods

Ethics statement

All experiments in this study were approved and performed in accordance with the guidelines from the Swedish National Board for Laboratory Animals and the European Community Council Directive (86/609/EEC) and the local ethics committee of Stockholm North. All efforts were made to minimize animal suffering and discomfort.

Animals

Cx3cr1^{CreER} (Jax Stock: 021160) and *Rosa26*^{DTA} (Jax Stock: 010527) mice were purchased from the Jackson Laboratory and bred to obtain both *Cx3cr1*$^{CreER/+}$*Rosa26*$^{DTA/+}$and *Cx3cr1*$^{CreER/+}$mice that were used for experiments. *C57BL/6* mice were bred in the Comparative Medicine Department at Karolinska University Hospital, Sweden. All experimental mice were maintained under regulated light/dark schedule and temperature conditions of this specific pathogen-free animal facility. All experimental mice were aged between 5–13 weeks-old and had free access to standard rodent chow and water.

Tamoxifen treatment

In order to induce the Cre recombinase in the *Cx3cr1*$^{CreER/+}$*Rosa26*$^{DTA/+}$mice, treatment with tamoxifen (TAM; Sigma, T5648–1G, St Louis, USA) was conducted when mice were 5–7 weeks old. Tamoxifen was resuspended in corn oil (Sigma, C8267–500ML, St Louis, USA) at 75°C for at least 60 min. The *Cx3cr1*$^{CreER/+}$*Rosa26*$^{DTA/+}$and *Cx3cr1*$^{CreER/+}$mice were administered 5mg (200μl) TAM subcutaneously on three consecutive days for microglial depletion, and then kept for one month to permit microglial repopulation, as we previously described [21, 22].

EAE induction and clinical evaluation

EAE was induced based on the standard protocol in our lab [25]. Briefly, MOG (amino acids 1–125 from the N terminus) was expressed in *Escherichia coli* and purified to homogeneity by chelate chromatography. Purified MOG dissolved in 6M urea was then dialyzed against sodium acetate buffer (10mM, pH 3.0) to obtain a soluble preparation. Mice were anesthetized with isoflurane (Forane; Abbott Laboratories, Abbot Park, IL) and injected subcutaneously in the dorsal tail base with 35μg of MOG in phosphate-buffered saline (PBS) emulsified in Complete Freund's Adjuvant (CFA, Chondrex, Inc, 7027, Redmond, USA) containing 100μg heat-killed Mycobacterium tuberculosis H37Ra (Difco Laboratory, Detroit, MI, USA). On the day of immunization and 48h later, mice were injected intraperitoneally with 200ng pertussis toxin (Sigma, P7208–50UG, St Louis, USA). Body weight and paralytic symptoms were assessed daily from 8 days post-immunization. The clinical signs of EAE were scored according to the following criteria: 0, no clinical signs of EAE; 1, tail weakness or tail paralysis; 2, hindlimb paraparesis or hemiparesis; 3, hindlimb paralysis or hemiparalysis; 4, tetraplegia or moribund; and 5, death (0.5 being assigned for intermediate clinical signs). The cumulative score was calculated as the sum of the daily scores of individual mice from day 0 until the day of termination. The clinical symptoms were scored in a blinded manner by 3 independent researchers.

Preparation of single cell suspensions from spleen and CNS

Mice were deeply anaesthetized by injecting 100µg pentobarbital intraperitoneally. Spleen were dissected and cell suspensions were prepared by mechanical dissociation in ice-cold PBS passing through 40µm cell strainers (734–0002, VWR). Mice were perfused through the left cardiac ventricle using ice-cold PBS. Whole brain and spinal cord were removed and minced using a surgical disposable scalpel (Medicarrier AB), followed by enzymatic digestion using Collagenase (11088866001, Roche) and DNAse (000000010104159001, Roche). Myelin was removed using a 38% Percoll gradient (P1644–1L, Sigma).

Flow cytometry

Single cell suspensions were plated into 96-well V-bottom plates and stained at 4°C for 20 min. Dead cells were removed using Live/Dead^{TM} Fixable Near-IR Dead Cell Stain Kit (Invitrogen, Thermo Fisher Scientific) in each panel. The following antibody panels were used: *1.* For myeloid cells analysis, single cell suspensions were incubated with Percp-Cy5.5-CD11b (clone: M1/70, BioLegend), PE/Cy7-CD45 (clone: 30-F11, BioLegend), PE-Ly6C (clone: HK1.4, BioLegend), V450-Ly6G (clone: 1A8, BD Biosciences), APC-F4/80 (clone: BM8, BioLegend), Alexa Fluor700-MHCII (clone: M5/114.15.2, BioLegend). 2. For T cells analysis, single cell suspensions were incubated with FITC-CD4 (clone: RM4–5, BD Biosciences), PE-CD8 (clone: 53–6.7, eBioscience), Percp-Cy5.5-CD3 (clone: 145–2C11, BioLegend), APC-CD62L (clone: MEL–14, eBioscience), Alexa Fluor700-CD44 (clone: IM7, BioLegend), PE/Cy7-Foxp3 (clone: FJK–16s, eBioscience) and V450-Ki67 (clone: B56, BD Biosciences). *3.* In order to measure intracellular cytokines, brain cells were seeded into 96-well plates with 200 µl of complete Dulbecco's Modified Eagle Medium (DMEM) containing 10% fetal bovine serum (BCCB2249, Sigma), penicillin-streptomycin (048M4774V, Sigma), L-glutamine (G7513, Sigma), 2-mercaptoethanol (Gibco by Life Technologies) and sodium pyruvate (11360039, Thermo Fisher Scientific) and stimulated with Ionomycin (I0634–1MG, Sigma-Aldrich), PMA (P1585–1MG, Sigma-Aldrich) and GolgiPlug (555029, BD Biosciences) for 5–6 hours. Afterwards, brain cells were first incubated with Alexa PCP5.5-CD4 (clone: GK15, BioLegend), PE/Cy7-CD8 (clone: 53–6.7, BioLegend) and A700-CD3 (clone: 17A2, BioLegend). Then cells were treated with fixation/permeabilization buffer (eBioscience) at least 30 min and followed by intracellular staining Fluor488-IL–4 (clone: 11B11, BioLegend), PE-IL–17 (clone: TC11–18H10, BD Biosciences) and APC-IFN-γ (clone: XMG1.2, BD Biosciences). Cells were acquired using a Gallios flow cytometer (Beckman Coulter) and analyzed using Kaluza software (Beckman Coulter).

CNS Histology and Immunohistochemistry

Brain and spinal cord tissues were dissected after perfusion using ice-cold PBS, and then immersed in 4% paraformaldehyde (PFA, Histolab) overnight, followed by dehydration with 30 % sucrose in 0.1M phosphate buffer at 4°C. Immunohistochemistry of the hemi-brain tissues was conducted in free-floating sections. Brain tissues were sectioned into 25µm slides using a Leica SM 2010 R Sliding Microtome (or a Leica SM 2000 R Sliding Microtome) and stored in tissue cryoprotectant solution (25% ethylene glycol and 25% glycerin in 0.1M phosphate buffer). Sections were washed in Tris-buffered saline (TBS, 50mM

Tris-HCl in 150mM NaCl, pH 7.5) and then blocked with 3% donkey serum in TBS with 0.1% Triton X–100 under moderate shaking. After blocking brain sections were incubated overnight with the following primary antibodies: Goat anti-Iba–1, 1:500 (ab5076, Abcam) and Rabbit anti-Tmem119, 1:500 (ab209064). Thereafter, sections were rinsed with TBS and incubated for 2 hours at room temperature with the indicated second antibodies (Donkey anti Goat, 1:1000, Alexa Fluor 633, 20127 BIOTIUM; Donkey anti-rabbit, 1:1000, Alexa Fluor 555, Invitrogen) together with Hoest (1:1000, 33342 Life Technologies). Sections were mounted and coverslipped using ProLong® Gold anti-fade reagent (1925239 Invitrogen). Spinal cord tissues sections (25µm thick) were prepared using a Leica CM3050 S Research Cryostat (or Leica CM1850 Research Cryostat) and mounted onto Superfrost® glass slides. Fluorescent images were captured using a LSM700 laser scanning confocal microscope (Axio-observer Z1; CarlZeiss microscopy, Germany), and analyzed using ZEN software (the black edition; Zeiss).

Statistical analysis

Severity of EAE was analyzed using a two-way analysis of variance (ANOVA). Two-tailed Student's t-test was used for direct comparison of two groups. One-way ANOVA and Tukey's multiple comparison tests were used to determine significance between more than two groups. Error bars are presented as SEM. Differences at $p<0.05$ were considered to be statistically significant. Statistical analysis was conducted using GraphPad software 8 (San Diego, CA).

Results

Long-term engraftment of microglia-like cells in Cx3cr1$^{CreER/+}$Rosa26$^{DTA/+}$ mice

In order to investigate the kinetic changes of microglial depletion and repopulation *Cx3cr1*$^{CreER/+}$*Rosa26*$^{DTA/+}$and *Cx3cr1*$^{CreER/+}$ mice were terminated at different time points (day 1, 3, 7 and 1 month) after three consecutive subcutaneous tamoxifen injections (experimental design depicted in Figure 1A). Flow cytometric and immunohistochemical analyses of brain and spinal cord tissues were performed at each time point. Approximately 92% of CD11b^{+}CD45^{low}Ly6C^{-}Ly6G^{-} microglia in the brain (gating strategy shown in Supplementary Figure 2A) could be depleted effectively 7 days after tamoxifen injections. The repopulation of microglia-like cells with two subpopulations, deriving from both the proliferation of residual CNS resident microglia and the engraftment of peripheral monocyte-derived microglia-like cells [21], was evident in the brain one month later (Figure 1B and D). Consistent with the findings in the brain, spinal cord CD11b^{+}CD45^{low}Ly6C^{-}Ly6G^{-} microglia (gating strategy shown in Supplementary Figure 2C) in *Cx3cr1*$^{CreER/+}$*Rosa26*$^{DTA/+}$mice could also be depleted effectively 7 days after tamoxifen injections, and repopulating microglia-like cells were noted one month later (Figure 1C and E). No depletion of microglia was noted in either the brains or spinal cords of *Cx3cr1*$^{CreER/+}$ mice, indicating their suitability as a control group (Figure 1B and C). We further confirmed these findings by

double immunofluorescent staining with Iba1and Tmem119 antibodies in both brain and spinal cord tissues at different time points (Figure 2A and 2B). In summary, the engraftment of microglia-like cells occurs in both the brain and spinal cord of *Cx3cr1*$^{CreER/+}$Rosa26$^{DTA/+}$ mice one month after administration of tamoxifen.

Female Cx3cr1$^{CreER/+}$Rosa26$^{DTA/+}$ mice develop more severe EAE after*engraftment of microglia-like cells*

EAE was induced by active immunization with MOG one month after tamoxifen injections in Cx3cr1$^{CreER/+}$Rosa26$^{DTA/+}$miceand Cx3cr1$^{CreER/+}$ mice, a time point when the CNS niche was colonized by microglia derived from both CNS microglia and peripherally-derived macrophages. In female Cx3cr1$^{CreER/+}$Rosa26$^{DTA/+}$ mice the disease onset was normal but a higher chronic disease severity was recorded than in male mice (Figure 3A, **P<0.01). In contrast, similar clinical scores during the whole EAE observation period were apparent in male and female Cx3cr1$^{CreER/+}$ control mice (Figure 3A). Furthermore, female Cx3cr1$^{CreER/+}$Rosa26$^{DTA/+}$mice had higher peak scores than did male mice (Figure 3 B, *P<0.05), while accumulative scores and day of disease onset were similar between groups. Overall, female Cx3cr1$^{CreER/+}$Rosa26$^{DTA/+}$ mice developed a more severe EAE course following engraftment of microglia-like cells.

In order to further explore if the engraftment of microglia-like cells contributed to disease severity during the EAE recovery period, tamoxifen was administered at days 8–10 post-immunization, allowing microglia-like cells to gradually repopulate after the clinical peak of EAE (Figure 3C). Again, female Cx3cr1$^{CreER/+}$Rosa26$^{DTA/+}$ mice also experienced a higher severity of the disease than did male mice, while this phenomenon was not evident in Cx3cr1$^{CreER/+}$ control mice of either gender (Figure 3C).

To exclude that this sex-specific effect of the engraftment of microglia-like cells was not due to a baseline gender difference in EAE development, we also compared the disease courses of male and female mice from different strains. Our results demonstrate that both males and females, irrespective of their strain background, develop similar EAE courses (Figure 3D). Taken together, we conclude that engraftment of peripherally-derived microglia-like cells in females exacerbates EAE disease.

CNS myeloid cell compositions during chronic EAE

We further confirmed that the gender differences in EAE severity were not dependent on the overall number of repopulating microglia in Cx3cr1$^{CreER/+}$Rosa26$^{DTA/+}$mice (Supplementary Figure 3). In order to analyze sex differences of CNS myeloid cell compositions during chronic EAE stage, brain and spinal cord tissues were dissected one month post-immunization (schematic overview is depicted in Figure 4A). Myeloid cell compositions in the brain and spinal cord tissues of Cx3cr1$^{CreER/+}$Rosa26$^{DTA/+}$mice and Cx3cr1$^{CreER/+}$ mice were analyzed using flow cytometry. The gating strategies of brain and spinal cord

myeloid cells are depicted in Supplementary Figures 2B and Figure 3B, respectively. We observed that infiltrating $CD11b^{+}CD45^{hi}Ly6C^{-}Ly6G^{-}$ macrophages, $Ly6C^{+}$ monocytes and $Ly6G^{+}$ neutrophils were still present in the CNS tissues during the chronic EAE stage (Figure 4B, C, F and G). Infiltrating $CD11b^{+}CD45^{hi}Ly6C^{-}Ly6G^{-}$ macrophages in the brain did not differ among different groups (Figure 4D), while increased numbers of $CD11b^{+}CD45^{hi}Ly6C^{-}Ly6G^{-}$ macrophages were recorded in the spinal cord of female mice (Figure 4E). The percentage of infiltrating $Ly6C^{+}$ monocytes and $Ly6G^{+}$ neutrophils in chronic EAE brains and spinal cords did not differ between $Cx3cr1^{CreER/+}Rosa26^{DTA/+}$ and $Cx3cr1^{CreER/+}$ mice or between sexes (Figure 4H and I).

Higher MHCII expression of infiltrating $Ly6C^{hi}$ monocytes during peak EAE in female microglia- repopulated mice

We next explored gender differences of CNS myeloid cells during the acute EAE stage. Brain and spinal cord tissues were thus dissected on day 18 post-immunization (schematic overview is depicted in Figure 5A) and gender differences were also noted in this setting (Figure 5B and C). Consistent with previous EAE results, there was a trend that following engraftment of microglia-like cells in female $Cx3cr1^{CreER/+}Rosa26^{DTA/+}$ mice worse clinical symptoms developed than in $Cx3cr1^{CreER/+}$ mice with resident microglia (Figure 5B). $Cx3cr1^{CreER/+}Rosa26^{DTA/+}$ female mice had an earlier disease onset than that of female control mice, and both peak score and accumulative scores were significantly higher than in female control mice (Figure 5B), while the corresponding male groups were comparable (Figure 5C). Furthermore, $CD11b^{+}CD45^{low}Ly6C^{-}Ly6G^{-}$ microglia in both the brain and spinal cord were less numerous in microglia-like cell engrafted groups than in control groups. Infiltrating $CD11b^{+}CD45^{hi}Ly6C^{-}Ly6G^{-}$ macrophages in the brain EAE tissues did not differ among groups, while the number of infiltrating $Ly6G^{+}$ neutrophils in EAE brains was significantly increased in the female repopulated microglia group than in the female control group (Figure 5D). Proportions of infiltrating $Ly6C^{+}$ monocytes and $Ly6G^{+}$ neutrophils in EAE spinal cord tissues did not differ among groups during the acute EAE period (Figure 5D). Importantly, MHCII expression of infiltrating $Ly6C^{hi}$ monocytes was significantly increased in female repopulated microglia mice than in the male group during the acute EAE period, but not during the chronic EAE period (Figure 5E).

Elevated cytokine production during EAE peak in female microglia-repopulated mice

In concert with the higher clinical score, we observed that the expression of IFN-γ in $CD4^{+}$ T cells ($CD4^{+}IFN\text{-}\gamma^{+}$ Tcell subgroup) was significantly greater in female $Cx3cr1^{CreER/+}Rosa26^{DTA/+}$ mice brains than in both the female control group and male $Cx3cr1^{CreER/+}Rosa26^{DTA/+}$ brains during the acute EAE stageFigure 6 A and B). Furthermore, the expression of IL−17 in $CD4^{+}$ T cells ($CD4^{+}IL-17^{+}$ Tcell

subgroup) was also significantly higher in female Cx3cr1$^{CreER/+}$Rosa26$^{DTA/+}$ brains when compared to female controlmice.Figure 6 C and D). Furthermore, no sex differences in numbers of infiltrating T cells in the brain (18 days post-immunization of EAE) were noted in Cx3cr1$^{CreER/+}$Rosa26$^{DTA/+}$ mice and Cx3cr1$^{CreER/+}$mice (Supplementary Figure 4). These data suggest that higher cytokine production in the female brain microenvironment in mice with microglia-like cells contributed to the gender-dependent exacerbation of EAE.

Discussion

In this study we utilized the Cx3cr1$^{CreER/+}$Rosa26$^{DTA/+}$ mice model which has the advantage of no need of invasive administration of diphtheria toxin, as is the case in the Cx3cr1$^{CreER:}$iDTR animal model [18]. Our previous studies using this model demonstrated that newly repopulating microglia are a combination of repopulation from both self-renewing de facto microglia and of infiltrating monocytes that become microglial-like transcriptionally [21, 23]. In the present study we addressed the functionality of these engrafted microglia-like cells in the setting of neuroinflammatory EAE disease, and noted their reduced ability to limit pathology compared to self-renewing microglia. The functional loss of microglial homeostasis or microglial trophic factors is thus not beneficial for EAE disease recovery. The significantly increased injury was sex-dependent with females experiencing worse pathology. This suggests that there are sex-specific differences in microglia-like cells. Recent data obtained from additional preclinical models also indicated that the number and phenotype of microglia may differ between females and males [26]. Given that microglial functional differences may predispose to previously underestimated but marked sex-dependent microglial activation patterns and signaling cascades in settings of CNS damage [27], it is tempting to speculate that the apparent preponderance of human MS among females is also at least in part attributable to their increased microglial dysfunctionality.

The timing of microglial ontogeny and development places them in a special position compared with other tissue resident macrophages. Microglia can be self-maintained by local proliferation and apoptosis with little contribution from circulating elements in physiological conditions. We and others have previously indicated that peripherally-derived macrophages can give rise to engrafted long-lived microglia-like cells in the brain parenchyma using experimental models, while remaining distinct gene signatures and functional differences such as phagocytic capacity and in vitro challenges [21, 24, 28]. The functional differences between these engrafted microglia-like cells and yolk sac-derived resident microglia in vivo thus have clinical implications for the treatment of diverse neurological diseases, as we previously reviewed [29].

Recent data indicated that microglial repopulation following experimental depletion using pharmacological colony-stimulating factor 1 receptor (CSF1R) inhibition could effectively resolve inflammation and promote disease recovery after brain injury, without any apparent adverse effects [30]. Using the same approach, age-related spatial memory impairment, microglial cell densities and morphologies could be reversed by replacing primed microglia in aged mice with newly repopulated

microglia [31], and they are also crucial for CNS regeneration following pro-inflammatory microglial necroptosis in a focal demyelinated animal model [32]. Furthermore, bone marrow-derived microglia-like cells may be more efficient in clearing amyloid beta deposits than their CNS endogenous counterparts [33]. CSF1R inhibition-mediated repopulation largely promotes repopulation by self-renewing microglia, while engraftment of microglia-like cells occurs in our $Cx3cr1^{CreER/+}Rosa26^{DTA/+}$ mice.

Tamoxifen, a non-steroidal estrogen receptor modulator, is used as a hormone therapy drug for treating breast cancer. Previous studies have reported that low doses of tamoxifen may promote microglial polarization toward an anti-inflammatory phenotype in male mice following chronic hypoperfusion [34]. Some may argue that tamoxifen itself may exert confounding effects on EAE independent of microglia depletion and repopulation. We induced MOG-EAE almost one month after injecting tamoxifen, and this should minimize any potential impact of tamoxifen on disease development. In our study we also included EAE male and female mice that were not treated with tamoxifen, which developed similar clinical scores during EAE, suggesting no sex difference in wild-type mice. Taken together our data support the notion that the replacement of microglia by engraftment of microglia-like cells has a sex-specific consequence on development of autoimmune neuroinflammation.

Antigen presentation in the CNS can be performed by infiltrating cells during autoimmune neuroinflammation. In this study the gender-dependent EAE severity in $Cx3cr1^{CreER/+}Rosa26^{DTA/+}$ mice with engraftment of microglia-like cells may be partially due to their higher MHCII expression and cytokine production in the female CNS. Correlation with enhanced $CD4^+IFN\text{-}\gamma^+$ and $CD4^+IL-17^+$ functionality in female mice support this increased disease-promoting immune activity. There is a current notion that peripherally-derived macrophages could be used to reconstitute microglial defects and may have therapeutic potential for a range of CNS pathologies[29, 33]. Our study indicates that careful consideration of gender effects and of desired in vivo functionality should be taken in design of future microglial replacement therapies.

Conclusion

The engraftment of microglia-like cells following microglial depletion exacerbated EAE in females. An underestimated yet marked sex-dependent microglial activation pattern may exist in the injured CNS during EAE.

Abbreviations

MS: multiple sclerosis; CNS: central nervous system; DTR: diphtheria toxin receptor; EAE: experimental autoimmune encephalomyelitis; MOG: myelin oligodendrocyte glycoprotein; MHCII: major histocompatibility complex class II; CSF1R: colony-stimulating factor 1 receptor.

Declarations

Acknowledgements

We thank the staff at AKM for animal caretaking.

Authors' contributions

Jinming Han designed and conducted the experiments, analyzed the data, and drafted the manuscript. Keying Zhu designed and conducted the experiments. Kai Zhou designed and conducted the experiments. Ramil Hakim conducted the experiments and edited the manuscript. Sreenivasa Raghavan Sankavaram conducted the experiments. Klas Blomgren, Harald Lund, Xing-Mei Zhang, and Robert A. Harris conceived and designed the experiments, interpreted the data, edited the manuscript, and acquired funding for the study. All authors approved the manuscript before submission.

Funding

This work was supported by grants from the China Scholarship Council (Grant No. 201600160072 and 201700260280), the Swedish Medical Research Council, Neuroforbundet, Alltid Litt Stekere, HjärnFonden, AlzheimerFonden and BarnCancerFonden.

Availability of data and materials

All data used in this manuscript are available from the corresponding author upon reasonable request.

Ethics declarations

Ethics approval and consent to participate

All experiments in this study were approved and performed in accordance with the guidelines from the Swedish National Board for Laboratory Animals and the European Community Council Directive (86/609/EEC) and the local ethics committee of Stockholm North under the ethical permits N138/14 and updated 9328–2019.

Consent for publication

Not applicable

Competing interests

The authors declare that they have no competing interests.

References

1.Reich, D. S., C. F. Lucchinetti, and P. A. Calabresi, Multiple Sclerosis. N Engl J Med, 2018. 378(2): p. 169–180.

2.Hagemeyer, N., et al., Microglia contribute to normal myelinogenesis and to oligodendrocyte progenitor maintenance during adulthood. Acta Neuropathol, 2017. 134(3): p. 441–458.

3.Butovsky, O. and H. L. Weiner, Microglial signatures and their role in health and disease. Nat Rev Neurosci, 2018. 19(10): p. 622–635.

4.Parkhurst, C. N., et al., Microglia promote learning-dependent synapse formation through brain-derived neurotrophic factor. Cell, 2013. 155(7): p. 1596–609.

5.Wlodarczyk, A., et al., A novel microglial subset plays a key role in myelinogenesis in developing brain. EMBO J, 2017. 36(22): p. 3292–3308.

6.Luo, C., et al., The role of microglia in multiple sclerosis. Neuropsychiatr Dis Treat, 2017. 13: p. 1661–1667.

7.Song, W. M. and M. Colonna, The identity and function of microglia in neurodegeneration. Nat Immunol, 2018. 19(10): p. 1048–1058.

8.International Multiple Sclerosis Genetics, C., Multiple sclerosis genomic map implicates peripheral immune cells and microglia in susceptibility. Science, 2019. 365(6460).

9.Heppner, F. L., et al., Experimental autoimmune encephalomyelitis repressed by microglial paralysis. Nat Med, 2005. 11(2): p. 146–52.

10.Zrzavy, T., et al., Loss of 'homeostatic' microglia and patterns of their activation in active multiple sclerosis. Brain, 2017. 140(7): p. 1900–1913.

11.Masuda, T., et al., Spatial and temporal heterogeneity of mouse and human microglia at single-cell resolution. Nature, 2019. 566(7744): p. 388–392.

12.Jordao, M. J. C., et al., Single-cell profiling identifies myeloid cell subsets with distinct fates during neuroinflammation. Science, 2019. 363(6425).

13.Du, L., et al., Role of Microglia in Neurological Disorders and Their Potentials as a Therapeutic Target. Mol Neurobiol, 2017. 54(10): p. 7567–7584.

14.Fumagalli, M., et al., How to reprogram microglia toward beneficial functions. Glia, 2018. 66(12): p. 2531–2549.

15.Priller, J. and M. Prinz, Targeting microglia in brain disorders. Science, 2019. 365(6448): p. 32–33.

16.Lund, H., M. Pieber, and R. A. Harris, Lessons Learned about Neurodegeneration from Microglia and Monocyte Depletion Studies. Front Aging Neurosci, 2017. 9: p. 234.

17.Han, J., R. A. Harris, and X. M. Zhang, An updated assessment of microglia depletion: current concepts and future directions. Mol Brain, 2017. 10(1): p. 25.

18.Bruttger, J., et al., Genetic Cell Ablation Reveals Clusters of Local Self-Renewing Microglia in the Mammalian Central Nervous System. Immunity, 2015. 43(1): p. 92–106.

19.Cronk, J. C., et al., Peripherally derived macrophages can engraft the brain independent of irradiation and maintain an identity distinct from microglia. J Exp Med, 2018.

20.Willis, E. F., et al., Repopulating Microglia Promote Brain Repair in an IL–6-Dependent Manner. Cell, 2020. 180(5): p. 833–846 e16.

21.Lund, H., et al., Competitive repopulation of an empty microglial niche yields functionally distinct subsets of microglia-like cells. Nat Commun, 2018. 9(1): p. 4845.

22.Lund, H., et al., Fatal demyelinating disease is induced by monocyte-derived macrophages in the absence of TGF-beta signaling. Nat Immunol, 2018. 19(5): p. 1–7.

23.Zhu, K., et al., Absence of microglia or presence of peripherally-derived macrophages does not affect tau pathology in young or old hTau mice. Glia, 2020.

24.Cronk, J. C., et al., Peripherally derived macrophages can engraft the brain independent of irradiation and maintain an identity distinct from microglia. J Exp Med, 2018. 215(6): p. 1627–1647.

25.Zhang, X. M., et al., Adoptive transfer of cytokine-induced immunomodulatory adult microglia attenuates experimental autoimmune encephalomyelitis in DBA/1 mice. Glia, 2014. 62(5): p. 804–17.

26.Guneykaya, D., et al., Transcriptional and Translational Differences of Microglia from Male and Female Brains. Cell Rep, 2018. 24(10): p. 2773–2783 e6.

27.Rahimian, R., P. Cordeau, Jr., and J. Kriz, Brain Response to Injuries: When Microglia Go Sexist. Neuroscience, 2019. 405: p. 14–23.

28.Shemer, A., et al., Engrafted parenchymal brain macrophages differ from microglia in transcriptome, chromatin landscape and response to challenge. Nat Commun, 2018. 9(1): p. 5206.

29.Han, J., et al., Enforced microglial depletion and repopulation as a promising strategy for the treatment of neurological disorders. Glia, 2019. 67(2): p. 217–231.

30.Rice, R. A., et al., Microglial repopulation resolves inflammation and promotes brain recovery after injury. Glia, 2017. 65(6): p. 931–944.

31.Elmore, M. R. P., et al., Replacement of microglia in the aged brain reverses cognitive, synaptic, and neuronal deficits in mice. Aging Cell, 2018: p. e12832.

32.Lloyd, A. F., et al., Central nervous system regeneration is driven by microglia necroptosis and repopulation. Nat Neurosci, 2019. 22(7): p. 1046–1052.

33.Kawanishi, S., et al., Bone-Marrow-Derived Microglia-Like Cells Ameliorate Brain Amyloid Pathology and Cognitive Impairment in a Mouse Model of Alzheimer's Disease. J Alzheimers Dis, 2018. 64(2): p. 563–585.

34.Chen, Y., et al., Tamoxifen promotes white matter recovery and cognitive functions in male mice after chronic hypoperfusion. Neurochem Int, 2019. 131: p. 104566.

Figures

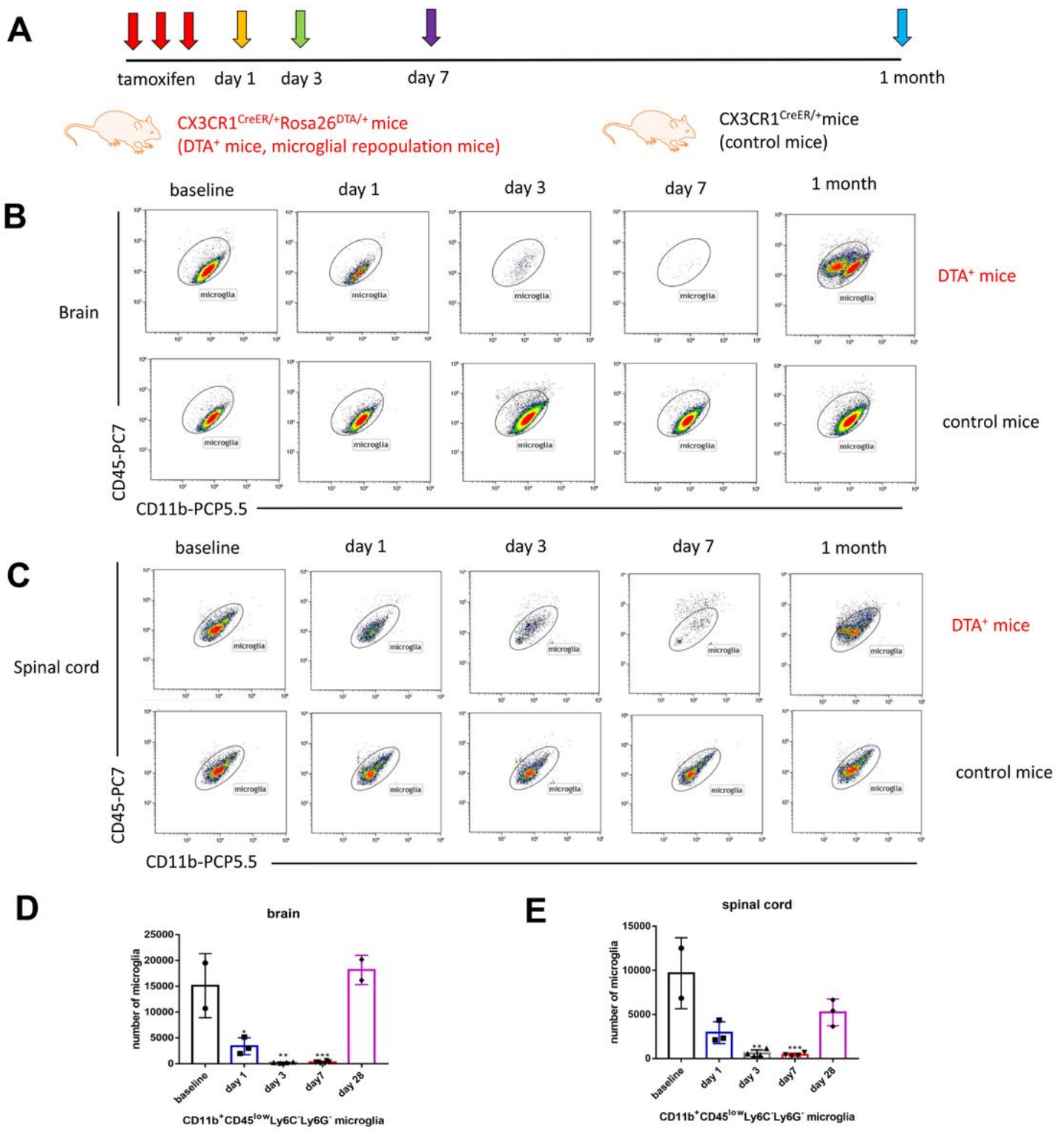

Figure 1

Long-term engraftment of microglia-like cells in Cx3cr1CreER/+Rosa26DTA/+ mice (A) Cx3cr1CreER/+Rosa26DTA/+ and Cx3cr1CreER/+ mice were sacrificed at different time points (day 1, 3, 7 and 1 month) following three consecutive subcutaneous tamoxifen injections. (B and C) Representative FACS plots of CD11b+CD45lowLy6C-Ly6G- microglia of the hemi-brains (B) and spinal cords (C) in Cx3cr1CreER/+Rosa26DTA/+ mice (microglial repopulated mice) and Cx3cr1CreER/+ mice (control mice)

are depicted during depletion and repopulation periods. (D and E) The individual values depict total CD11b+CD45lowLy6C-Ly6G- microglial counts (±SEM) of the hemi-brains (D) and spinal cords (E) in Cx3cr1CreER/+Rosa26DTA/+ mice during depletion and repopulation periods (baseline, black bars; day 1, blue bars; day 3, gray bars; day 7, red bars and 1 month, pink bars). Statistical significance is indicated as ∗p < 0.05, ∗∗p < 0.01 and ∗∗∗p < 0.001.

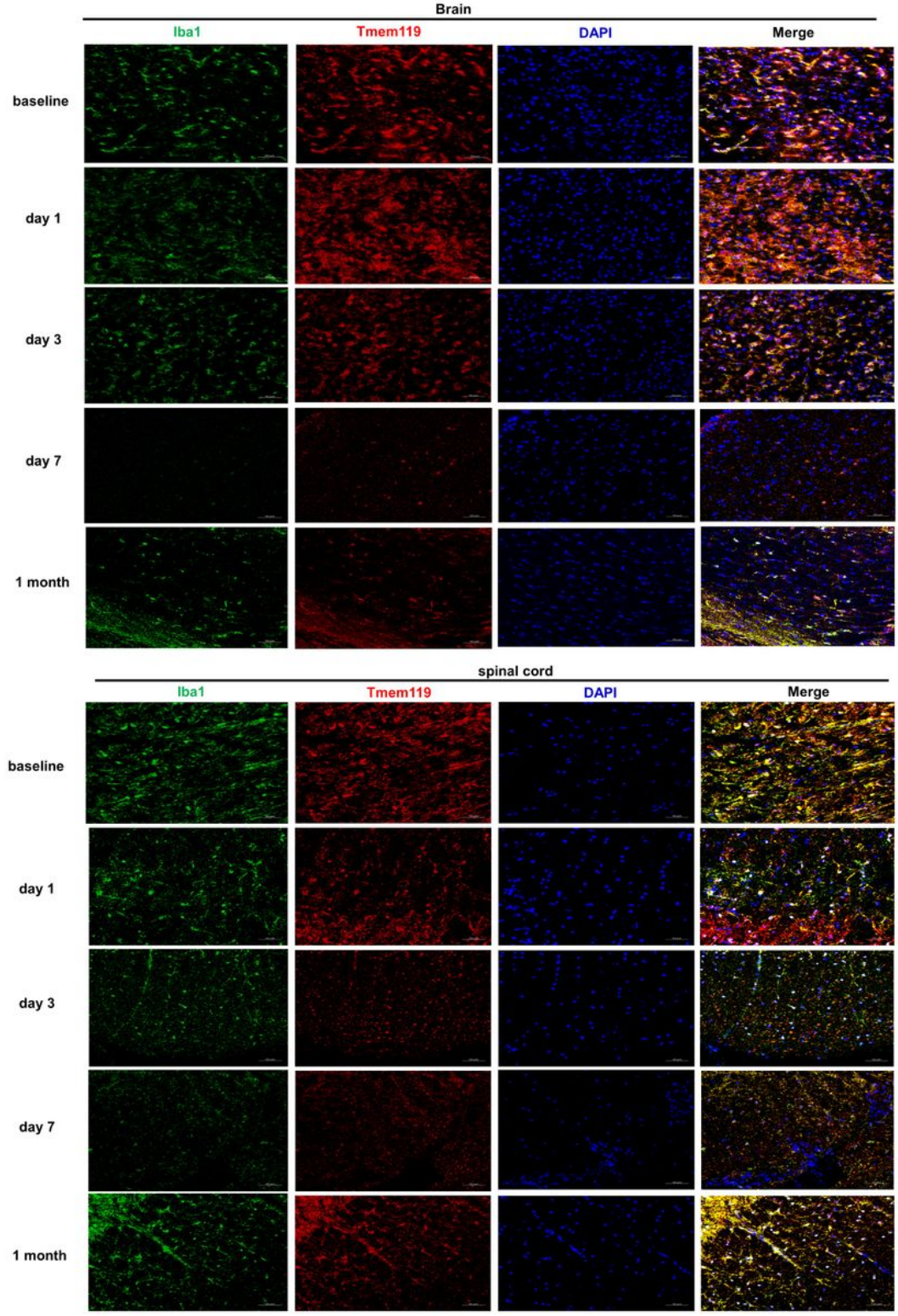

Figure 2

Microglia are effectively depleted by day 7 after tamoxifen injections and repopulated 1 month later in Cx3cr1CreER/+Rosa26DTA/+ mice. (A and B) An example of each time point (day 1, 3, 7 and 1 month) of double immunofluorescent staining of Iba1 (green) and Tmem119 (red) in the (A) hemi-brains and (B) spinal cords of Cx3cr1CreER/+Rosa26DTA/+ and Cx3cr1CreER/+Rosa26DTA/- mice followed by three consecutive subcutaneous tamoxifen injections. Scale bars represent 50 µm.

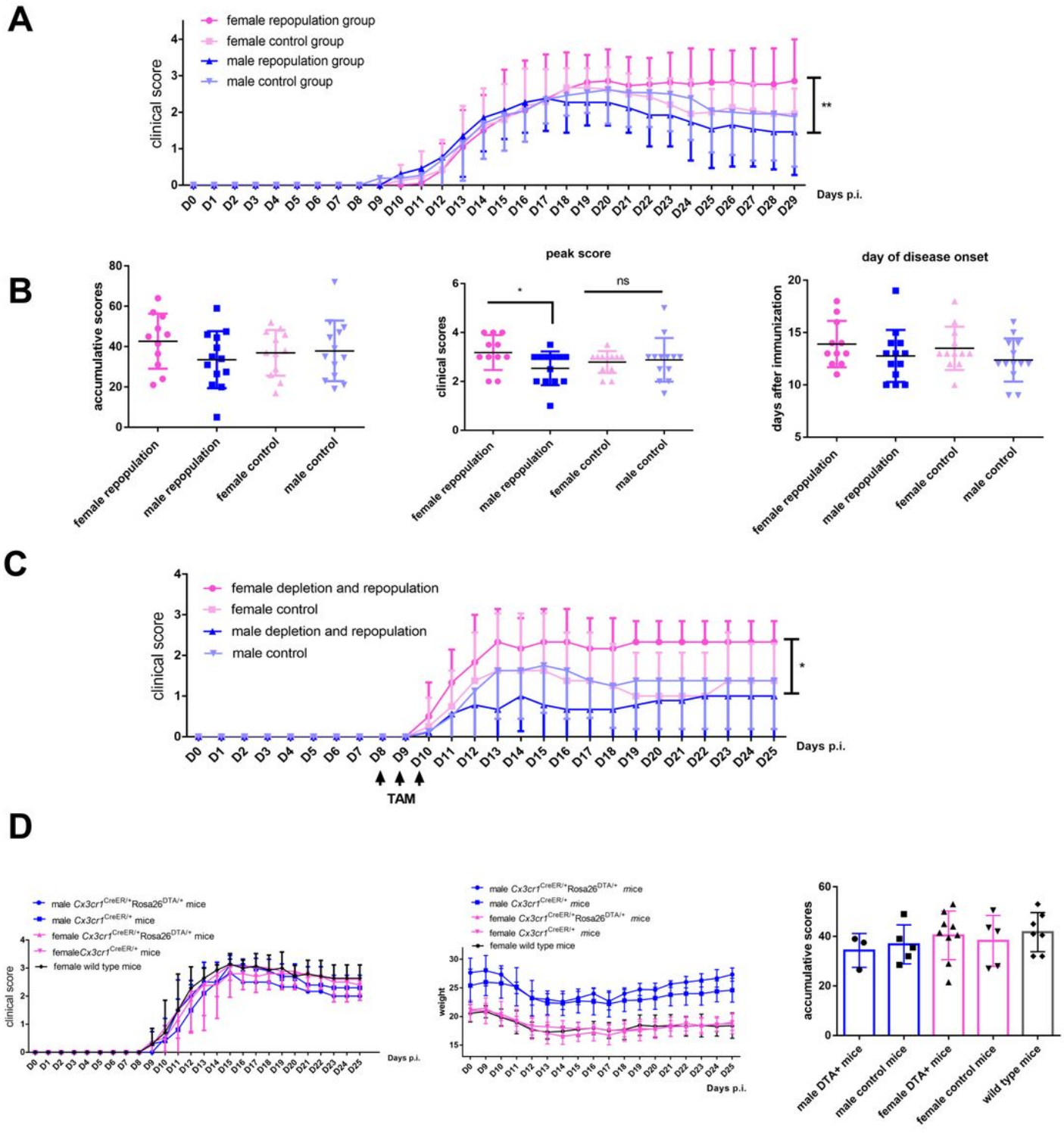

Figure 3

*Female Cx3cr1CreER/+Rosa26DTA/+ mice develop more severe EAE after engraftment of microglia-like cells (A) Tamoxifen was first administrated and EAE was subsequently induced when microglia are repopulated (one month later). Clinical scores of neurological deficits post-immunization up to 29 days are indicated. Female Cx3cr1CreER/+Rosa26DTA/+ mice with newly repopulated microglia (dark pink color) had a similar disease onset but experienced a higher disease severity at the chronic stage than did female Cx3cr1CreER/+ mice with resident microglia (light pink color, *P<0.05, pooled from two independent experiments). Male Cx3cr1CreER/+Rosa26DTA/+ mice with newly repopulated microglia (dark blue color) experienced similar clinical scores during the whole EAE period when compared with male Cx3cr1CreER/+ mice with resident microglia (light blue color, pooled from three independent experiments). (B) Peak disease score, day of disease onset and accumulative scores of both male and female groups are depicted during EAE. (C) EAE was first induced and tamoxifen was subsequently administrated at day 8, 9 and 10 post-immunization. Clinical scores of neurological deficits post-immunization up to 25 days are presented. (D) Different mice strains (Cx3cr1CreER/+Rosa26DTA/+ male and female mice, Cx3cr1CreER/+ male and female mice and C57BL/6 female wild-type mice) without tamoxifen injections developed similar clinical scores and accumulative scores during EAE course. Statistical significance is indicated as $*p < 0.05$, $**p < 0.01$ and $***p < 0.001$.*

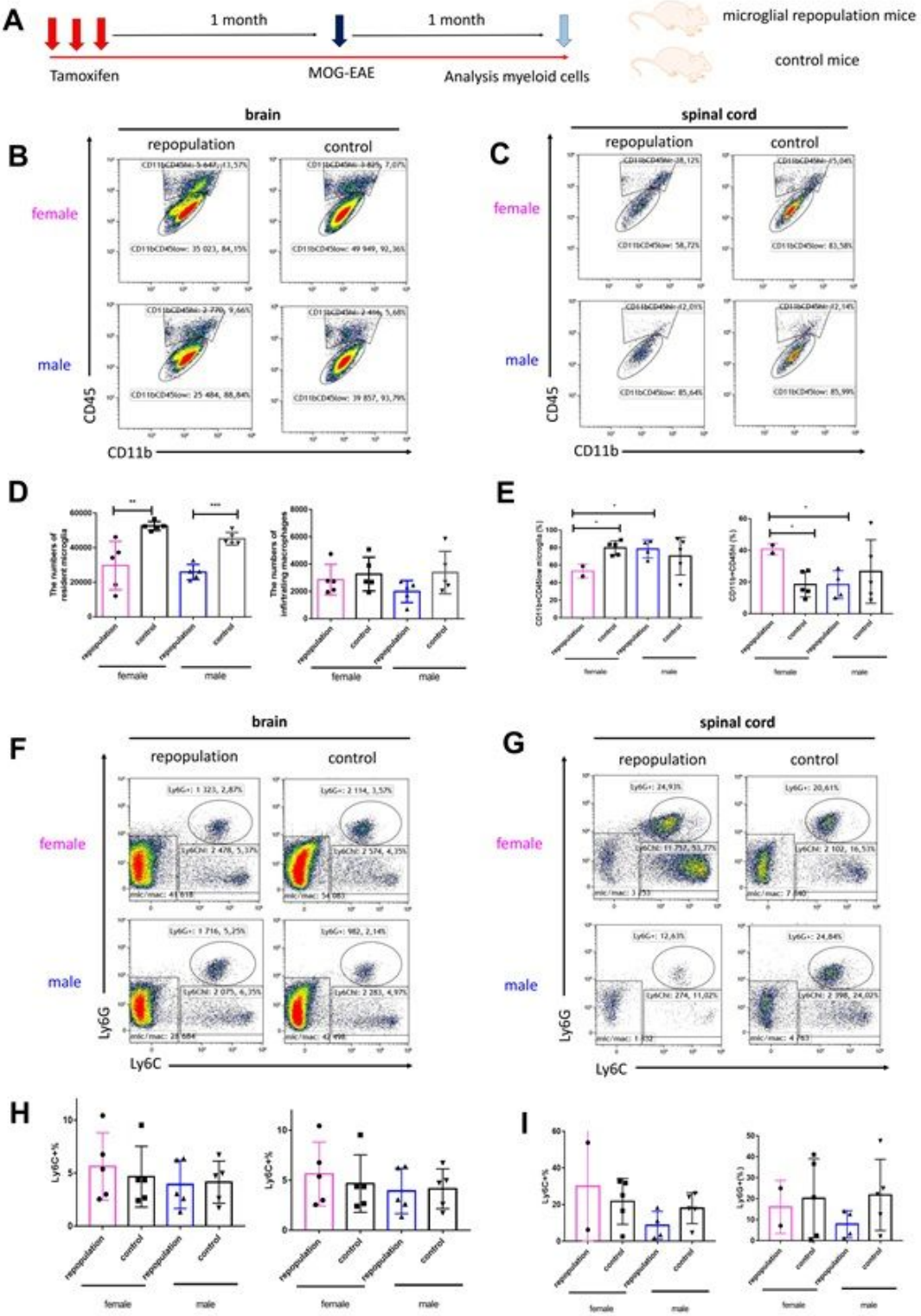

Figure 4

CNS myeloid cell compositions during chronic EAE (A) Schematic overview of the experimental design. One month after tamoxifen injections, EAE was induced by active immunization with MOG in Cx3cr1CreER/+Rosa26DTA/+ mice with newly repopulated microglia and Cx3cr1CreER/+Rosa26DTA/- with resident microglia (both male and female mice). Brain and spinal cord tissues were dissected on day 29 post-immunization (chronic EAE period). (B and C) Myeloid cell subsets analysis in the brain and

spinal cord tissues of the Cx3cr1CreER/+Rosa26DTA/+ mice and Cx3cr1CreER/+Rosa26DTA/- mice were performed using flow cytometry. (D) The numbers of CD11b+CD45lowLy6C-Ly6G- brain microglia in repopulated microglia groups are lower than in control groups and the numbers of infiltrating CD11b+CD45hiLy6C-Ly6G- macrophages in the brain EAE tissues did not differ among the different groups. (E) The percentage of CD11b+CD45lowLy6C-Ly6G- spinal cord microglia in female repopulated microglia group were lower than in the control group as expected, while infiltrating CD11b+CD45hiLy6C-Ly6G- macrophages in the spinal cord EAE tissues were significantly increased in the female repopulated microglia group. (F and G) Representative FACS plots of infiltrating Ly6C+ monocytes and Ly6G+ neutrophils in EAE brain and spinal cord tissues are depicted during the chronic EAE period. (H and I) Infiltrating Ly6C+ monocytes and Ly6G+ neutrophils in EAE brain and spinal cord tissues did not differ among different groups during chronic EAE period. Statistical significance is indicated as $*p < 0.05$, $**p < 0.01$ and $***p < 0.001$.

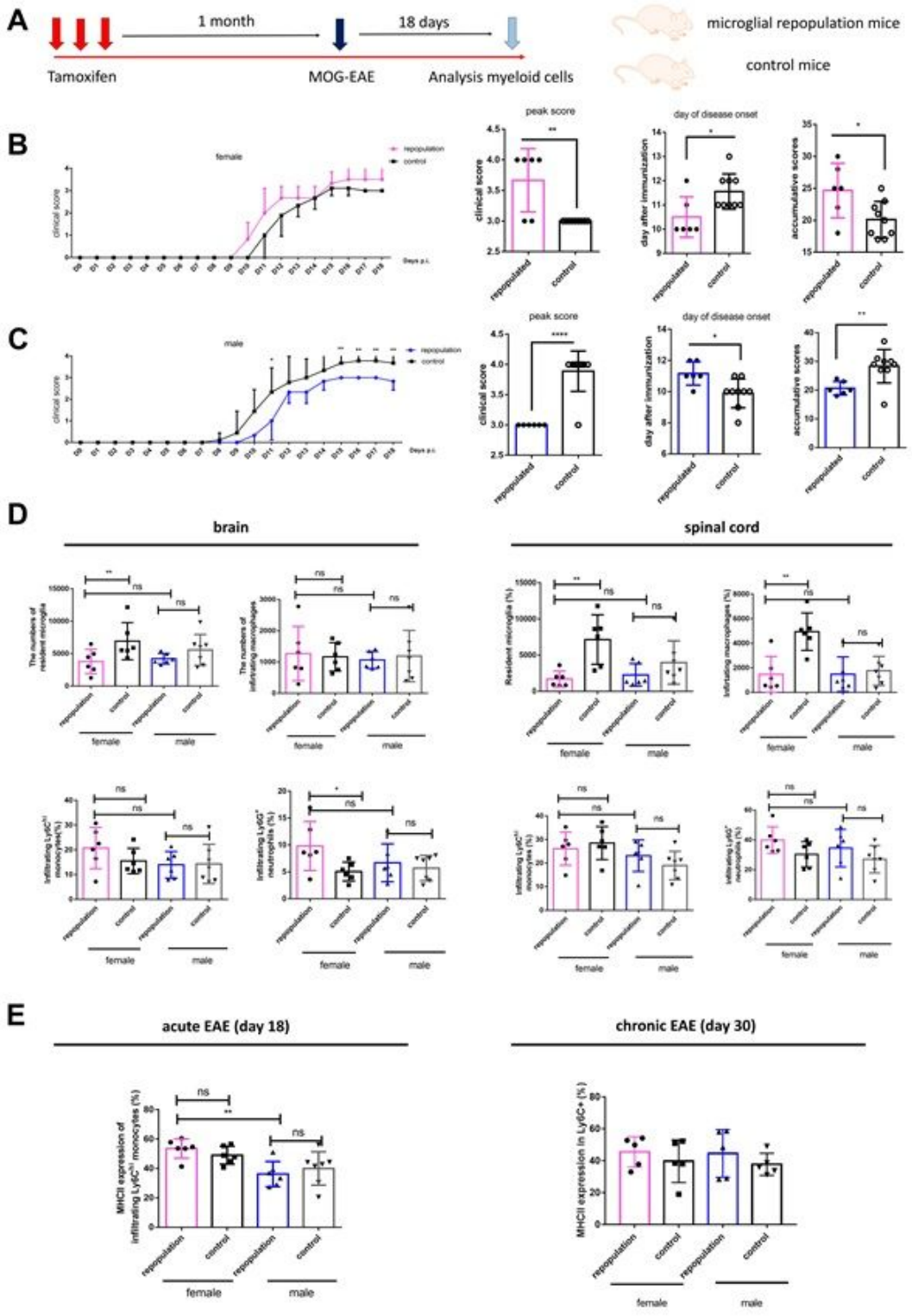

Figure 5

Higher MHCII expression of infiltrating Ly6Chi monocytes during EAE peak in female microglia-repopulated mice (A) Schematic overview of the experimental design. One month after tamoxifen injections, EAE was induced by active immunization with MOG in Cx3cr1CreER/+Rosa26DTA/+ with newly repopulated microglia and Cx3cr1CreER/+Rosa26DTA/- with resident microglia (both male and female mice). Brain and spinal cord tissues were dissected on day 18 post-immunization (acute EAE

period). (B and C) Clinical scores of neurological deficits post-immunization up to 18 days are indicated. Peak disease score, day of disease onset and accumulative scores of both male and female groups are depicted. (D) Myeloid cell subsets analysis in the brain and spinal cord tissues of Cx3cr1CreER/+Rosa26DTA/+ mice and Cx3cr1CreER/+Rosa26DTA/- mice were performed by using flow cytometry during the chronic EAE disease course. (E) MHCII expression (%) of infiltrating Ly6Chi monocytes was increased more in the female repopulated microglia group than in the male repopulated group during the acute EAE period, while significant differences were not evident during the chronic EAE period. Statistical significance is indicated as $*p < 0.05$, $**p < 0.01$ and $***p < 0.001$.

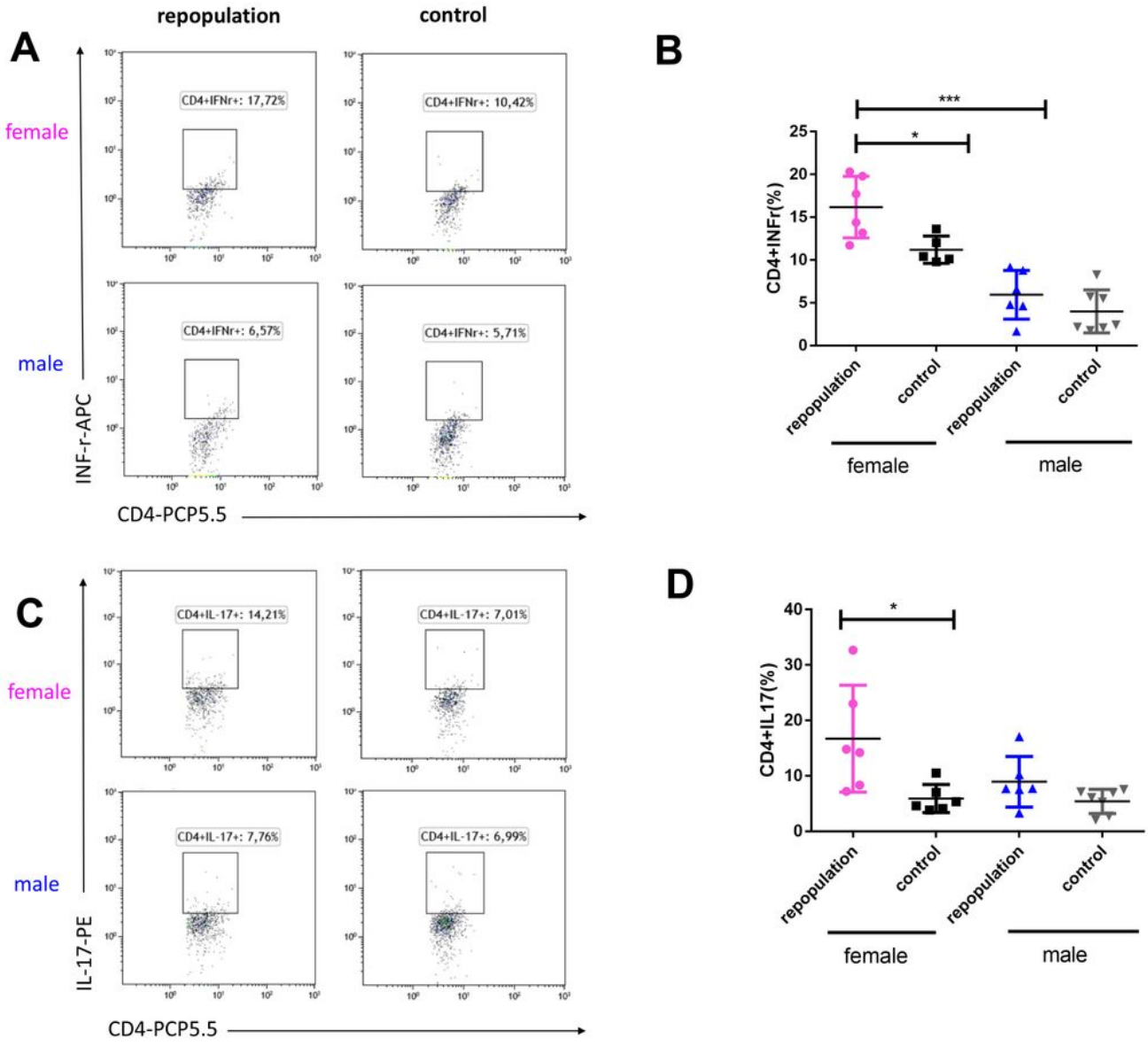

Figure 6

Elevated cytokine production during EAE peak in female microglia-repopulated mice (A) FACS data showing the expression of IFN-⍰⍰ in CD4+ T cells from the brains of Cx3cr1CreER/+Rosa26DTA/+ and Cx3cr1CreER/+Rosa26DTA/- mice. (B and C) FACS data showing the expression of IL-17 in CD4+ T cells from the brains of Cx3cr1CreER/+Rosa26DTA/+ and Cx3cr1CreER/+Rosa26DTA/- mice. (D)

Representative numbers indicate the percentage of each compartment. Statistical significance is indicated as $*p < 0.05$, $**p < 0.01$ and $***p < 0.001$.